

PACS numbers: 42.55.Rz; 42.60.Da; 42.60.Mi; 42.65.Sf
DOI: 10.1070/QE2014v044n01ABEH015286

Synchronisation of self-oscillations in a solid-state ring laser with pump modulation in the region of parametric resonance between self-modulation and relaxation oscillations

V.Yu. Dudetskiy, E.G. Lariontsev, S.N. Chekina

Abstract. **The synchronisation of the self-modulation oscillation frequency in a Nd:YAG ring laser by an external periodic signal modulating the pump power in the region of parametric resonance between self-modulation and relaxation oscillations is studied theoretically and experimentally. The characteristic features of synchronisation processes in lasers operating in the self-modulation regime of the first kind and in the regime with a doubled self-modulation period are considered. Two bistable branches of synchronisation of self-modulation oscillations are found by numerical calculation. The experimental data agree well with the numerical simulation results for one of these branches, but the other branch of bistable self-modulation oscillations was not observed experimentally.**

Keywords: *solid-state ring laser, self-modulation oscillation regime, parametric resonance, frequency synchronisation, radiation bistability.*

1. Introduction

The synchronisation of self-modulation oscillations (SOs) in lasers was studied in a number of works (see, for example, [1–6]). One of the aims of these works was to study synchronisation as a fundamental phenomenon observed in dynamic systems of different natures [7]. The general case of synchronisation of periodic oscillations of the n/m order, in which the frequency Ω of synchronised SOs and the external modulation signal frequency ω relate as $n\omega = m\Omega$, was studied in [1–4]. The synchronisation of quasi-periodic SOs by an external periodic signal was studied in [5, 6]. The other problems that can be solved by the synchronisation of SOs by an external periodic signal are related to the control of oscillation dynamics and to the improvement of SO stability. Technical fluctuations (first of all, pump noise and instability of coupling coefficients of counterpropagating waves) lead to instability of the SO frequency, which can be considerably decreased by synchronisation of SOs by an external periodic signal.

V.Yu. Dudetskiy Department of Physics, M.V. Lomonosov Moscow State University, Vorob'evy gory, 119991 Moscow, Russia; e-mail: vadim.dudetskiy@gmail.com;
E.G. Lariontsev, S.N. Chekina D.V. Skobel'tsyn Institute of Nuclear Physics, M.V. Lomonosov Moscow State University, Vorob'evy gory, 119991 Moscow, Russia; e-mail: e.lariontsev@yahoo.com

Received 17 July 2013; revision received 2 October 2013
Kvantovaya Elektronika **44** (1) 23–29 (2014)
Translated by M.N. Basieva

SOs in solid-state ring lasers (SSRLs) are usually excited as a result of competition of counterpropagating waves. There is a number of possible self-modulation oscillation regimes (see review [8] and papers [9–11]), the main and most frequent regime among them being the SOs of the first kind. Previously, the theory of synchronisation of SOs in SSRLs by an external periodic signal was developed in [12] and the synchronisation of SOs of the first kind with periodic modulation of pump power was studied experimentally in [2, 3, 6].

As is known, the self-modulation regime of the first kind is stable only out of the region of parametric resonance between self-modulation and relaxation oscillations [13]. In the parametric resonance region, this regime is changed by a self-modulation regime with a doubled period of oscillations and by other regimes. In the case of symmetric coupling of counterpropagating waves (at identical coupling coefficient magnitudes, $m_1 = m_2$), the width of the parametric resonance region turns to zero. In the case of asymmetric coupling of counterpropagating waves, the parametric resonance range considerably extends with increasing difference between the coupling coefficient magnitudes of the counterpropagating waves $m_1 - m_2$ [13].

Note that the synchronisation was previously studied only for the self-modulation regime of the first kind. The specific features of synchronisation for other self-modulation regimes occurring in the parametric resonance region have not yet been studied. The aim of the present work is to fill in this gap. In this work, we theoretically (based on numerical simulation) and experimentally study the synchronisation of SOs by an external periodic signal modulating the pump power in the region of parametric resonance between self-modulation and relaxation oscillations.

2. Experimental setup

The ring chip laser under study was designed as a monoblock in the form of a prism with one spherical face (radius of curvature 50 mm) and three plane total-internal-reflection faces. The geometric perimeter of the cavity was 2.8 cm, and the nonplanarity angle was 80°. The laser was pumped by a semiconductor laser diode at a wavelength of 0.810 μm. The laser diode power supply circuit included a generator of periodic oscillations, which modulated the pump power within the frequency range 50–220 kHz. The monoblock temperature was controlled by a thermal stabilisation system [6] so that the ratio of the feedback coefficient magnitudes of the counterpropagating waves was maximal ($m_1/m_2 = 2.$).

In the experiments, we measured the temporal and spectral characteristics of the intensity of counterpropagating

waves depending on the pump power excess over the threshold η_0, as well as on the frequency and amplitude of the signal modulating the pump power. The signals were recorded using a 20-12-PCI ADC and a broadband Tektronix TDS 2014 digital oscilloscope.

3. Theoretical model and laser parameters

The numerical simulation in this work was performed using a vector model of an SSRL [8, 14]. In this model the polarisation of counterpropagating waves is assumed to be given and determined by the unit vectors $\boldsymbol{e}_{1,2}$ for opposite directions. The initial system of equations of the vector model has the form

$$\begin{aligned}
\frac{\mathrm{d}}{\mathrm{d}t}\tilde{E}_{1,2} &= -\frac{\omega_c}{2Q_{1,2}}\tilde{E}_{1,2} \pm \mathrm{i}\frac{\Omega}{2}\tilde{E}_{1,2} + \frac{\mathrm{i}}{2}\tilde{m}_{1,2}\tilde{E}_{2,1} \\
&+ \frac{\sigma l}{2T}(N_0\tilde{E}_{1,2} + N_{\pm}\tilde{E}_{2,1}), \\
T_1\frac{\mathrm{d}N_0}{\mathrm{d}t} &= N_{\mathrm{th}}(1+\eta) - N_0 - N_0 a(|\tilde{E}_1|^2 + |\tilde{E}_2|^2) \\
&- N_+ a\tilde{E}_1\tilde{E}_2^* - N_- a\tilde{E}_1^*\tilde{E}_2, \\
T_1\frac{\mathrm{d}N_+}{\mathrm{d}t} &= -N_+ - N_+ a(|\tilde{E}_1|^2 + |\tilde{E}_2|^2) - \beta N_0 a\tilde{E}_1^*\tilde{E}_2 .
\end{aligned} \tag{1}$$

Here, $\omega_c/Q_{1,2}$ are the cavity bandwidths; $Q_{1,2}$ are the cavity Q factors for counterpropagating waves (hereinafter we take $Q_1 = Q_2 = Q$); $T = L/c$ is the round-trip time for a cavity with the length L; T_1 is the longitudinal relaxation time; l is the active element length; $a = T_1 c\sigma/(8\hbar\omega\pi)$ is the saturation parameter; σ is the laser transition cross section; $\Omega = \omega_1 - \omega_2$ is the frequency nonreciprocity of the cavity; ω_1 and ω_2 are the cavity eigenfrequencies for the counterpropagating waves; the pump rate is represented in the form $N_{\mathrm{th}}(1+\eta)/T_1$; N_{th} is the threshold inverse population; $\eta = P/P_{\mathrm{th}} - 1$ is the pump power excess over the threshold; $\tilde{E}_{1,2}(t) = E_{1,2}\exp(\mathrm{i}\varphi_{1,2})$ are the complex amplitudes of the fields of counterpropagating waves; and N_0, $N_{\pm}$ are the spatial harmonics of the inverse population N, which are determined by the expressions

$$N_0 = \frac{1}{L}\int_0^L N\mathrm{d}z, \quad N_{\pm} = \frac{1}{L}\int_0^L \boldsymbol{e}_1^*\boldsymbol{e}_2 N\exp(\pm\mathrm{i}2kz)\,\mathrm{d}z. \tag{2}$$

The system of equations (1) differs from the equations of the standard SSRL model [1] only by the presence of the polarisation factor

$$\beta = (\boldsymbol{e}_1\boldsymbol{e}_2)^2 = \cos^2\gamma, \tag{3}$$

where γ is the angle between the unit vectors $\boldsymbol{e}_{1,2}$.

The linear coupling of counterpropagating waves is determined by the phenomenologically introduced complex coupling coefficients

$$\tilde{m}_1 = m_1\exp(\mathrm{i}\vartheta_1), \quad \tilde{m}_2 = m_2\exp(-\mathrm{i}\vartheta_2), \tag{4}$$

where $\vartheta_{1,2}$ are the phases of the coupling coefficients $m_{1,2}$.

In the case of pump modulation, the pump power excess over the threshold is

$$\eta(t) = \eta_0 + h\sin(2\pi f_p t), \tag{5}$$

where η_0 is the pump excess over the threshold in the absence of modulation, while h and f_p are the pump modulation depth and frequency.

The numerical simulation was performed at the laser parameters close to the experimentally measured parameters of a Nd : Y AG ring chip laser [10]. The relaxation time was T_1 = 240 μs, and the cavity bandwidth was determined by the relaxation frequency $\omega_r = \sqrt{\eta\omega_c/QT_1}$. In the studied laser, the main relaxation frequency at $\eta_0 = 0.2$ is $\omega_r/2\pi$ = 98.5 kHz, which yields $\omega_c/Q = 4.37 \times 10^8$ s^{-1}. Similar to [14], the polarisation parameter $\beta = 0.75$ was determined by the experimentally measured dependence of the additional relaxation frequency ω_{r1} on the frequency nonreciprocity of the cavity Ω.

As was shown in [6], the ratio m_1/m_2 in a ring chip laser can be changed by changing the monoblock temperature. For numerical simulation, we chose m_1 = 1986400 s^{-1} and m_2 = 861378 s^{-1}. At these m_1 and m_2, the SO frequencies and the ratio of average intensities of the counterpropagating waves are close to the experimentally measured values. The phase difference of the complex coupling coefficients $\tilde{m}_{1,2}$ is difficult to estimate from the SO characteristics. For simplicity, the phase difference $\vartheta_1 - \vartheta_2$ was taken to be zero. It was also assumed that the ring cavity has no frequency and amplitude nonreciprocities ($\Omega = 0$, $\Delta = \omega_c/2Q_2 - \omega_c/2Q_1 = 0$).

4. Periodic and quasi-periodic synchronisation regimes

The self-contained ring chip lasers in a wide range of laser parameters (outside the parametric resonance region) can operate in the self-modulation regime of the first kind, which is characterised by a sinusoidal counter-phase modulation of the intensities of counterpropagating waves. This regime is stable only outside the parametric resonance region, between self-modulation and relaxation oscillations [10, 13]. In the parametric resonance region, the SO frequency is close to the doubled relaxation frequency ($\omega_m \approx 2\omega_r = 2\sqrt{\eta_0\omega_c/QT_1}$).

In this work, we varied the pump excess over the threshold η_0, as well as the pump power modulation depth h and frequency f_p. If the frequency f_p is close to the SO frequency f_m, synchronisation of SOs in a SSRL can occur, and the self-modulation frequency in this case is locked by the external signal: $f_m = f_p$. It is this synchronisation region that we consider. The synchronisation is also possible when the modulation frequencies f_p are close to $f_m/2$, as well as in the region of frequencies $f_p \cong 2f_m$. These synchronisation regions will be studied separately.

The experimental investigations and the numerical simulation were performed at several values of the pump excess over the threshold η_0. A change in η_0 leads to a change in the relaxation frequency ω_r. If the frequency $2\omega_r$ approaches the SO frequency ω_m, there appear some nonlinear effects related to the parametric interaction of self-modulation and relaxation oscillations (parametric resonance). In the region of parametric resonance, the self-modulation regime of the first kind becomes unstable and a SO period doubling bifurcation arises [10].

The modulation frequency f_p and depth h were varied at each η_0. It is found that, inside the parametric resonance region, variation of the controlling parameters η_0 and f_p can lead to several synchronisation regimes.

4.1. Numerical simulation results

In the absence of pump modulation, the self-modulation regime of the first kind is unstable and is transformed into the periodic self-modulation regime with a doubled modulation period in the pump excess region $0.23 \leqslant \eta_0 < 0.35$. Let us first consider the range $0.17 \leqslant \eta_0 < 0.23$, which is rather close to the instability boundary and in which the self-modulation regime of the first kind is still stable in the absence of modulation ($h = 0$). Numerical simulation showed that the synchronisation of SOs in this region can occur in two regimes, periodic and quasi-periodic. The SO frequency at $\eta_0 = 0.15$ was 214.5 kHz. The synchronisation of SOs appears in the frequency region $f_- \leqslant f_p \leqslant f_+$, where f_- and f_+ are the lower and upper boundaries of the synchronisation range. The periodic synchronisation regime exists in the frequency region near the upper synchronisation region boundary f_+, while the quasi-periodic regime exists near the lower boundary f_-.

Figure 1 shows the typical radiation intensity spectra for the periodic and quasi-periodic synchronisation of SOs. In the first case (Fig. 1a), as well as in the self-modulation regime of the first kind, the radiation spectra show only one spectral component, which corresponds to f_p, i.e., locking of the SO frequency takes place ($f_m = f_p$). In the quasi-periodic regime (Fig. 1b), the synchronisation of SOs manifests itself in the locking of the peak at f_m by the modulating signal frequency f_p. In addition, two more components appear in the spectrum at the frequency f_1 close to f_r and at the combination frequency $f_p - f_1$.

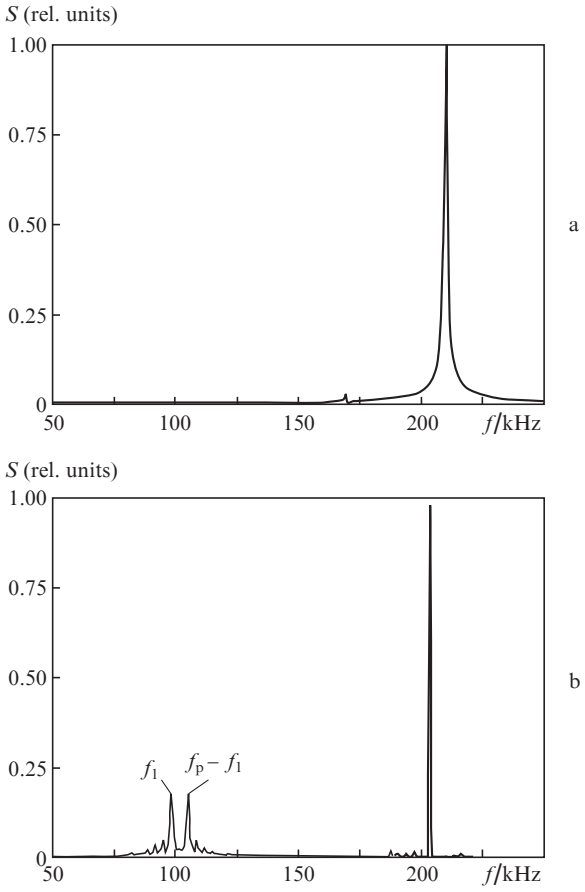

Figure 1. Numerically simulated radiation intensity spectra for the periodic (f_p = 210 kHz) (a) and quasi-periodic (f_p = 204 kHz) (b) regimes of synchronisation of SOs at $\eta_0 = 0.17$ and $h = 0.25$.

Figure 2 shows the regions of existence of the periodic and quasi-periodic synchronisation regimes at $\eta_0 = 0.15$ and 0.17 (pump modulation depth $h = 0.25$). For the quasi-periodic synchronisation regime, Fig. 2 presents two curves, one of them corresponding to the frequency $f_m = f_p$ and the second corresponding to the frequency f_1, which, inside the synchronisation region, linearly depends on f_p. As is seen from Fig. 2a, at $\eta_0 = 0.15$ the quasi-periodic regime only begins to arise, and the region of its existence occupies only a small part of the total synchronisation range. With increasing η_0, the existence region of the quasi-periodic synchronisation extends.

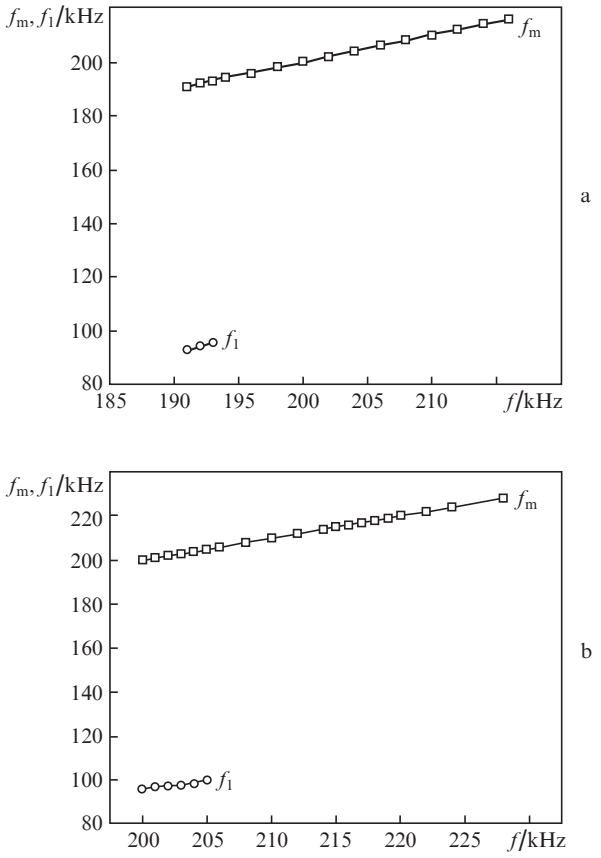

Figure 2. Existence regions of the periodic and quasi-periodic synchronisation regions found by numerical simulation at the pump excess over the threshold $\eta_0 = 0.15$ (a) and 0.17 (b); the modulation depth is $h = 0.25$.

4.2. Experimental results

Let us now consider our experimental results. Figure 3 presents a typical intensity spectrum of one of the waves in the vicinity of the SO frequency (at $\eta_0 = 0.15$) in the absence of pump modulation ($h = 0$), which shows that the SO frequency in the studied chip laser is unstable and exhibits fluctuations (spectral width about 5 kHz). In the synchronisation regimes, the width of the spectral component locked by the external signal ($f_m = f_p$) decreases by more than an order of magnitude (Fig. 3b).

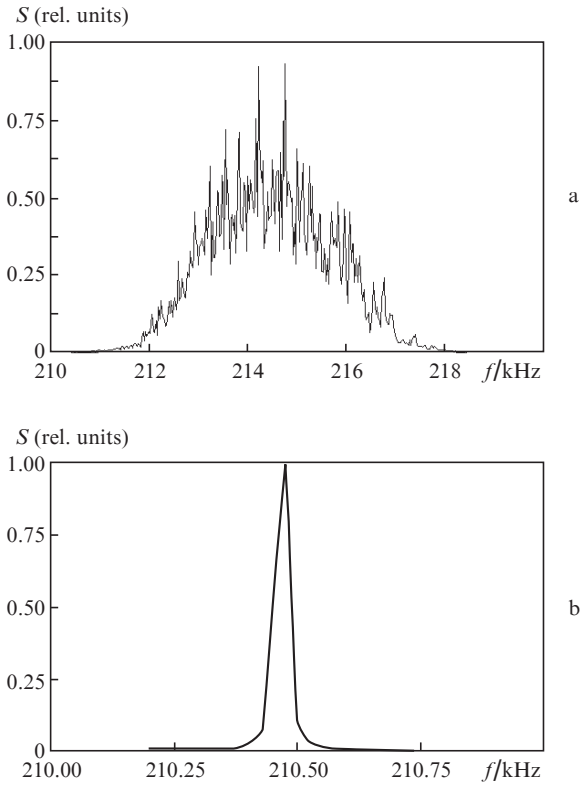

Figure 3. Line profile in the experimentally measured radiation spectra at $\eta_0 = 0.15$ in the absence of pump modulation (a) and in the periodic synchronisation regime at $f_p = 210.4$ kHz and $h = 0.25$ (b).

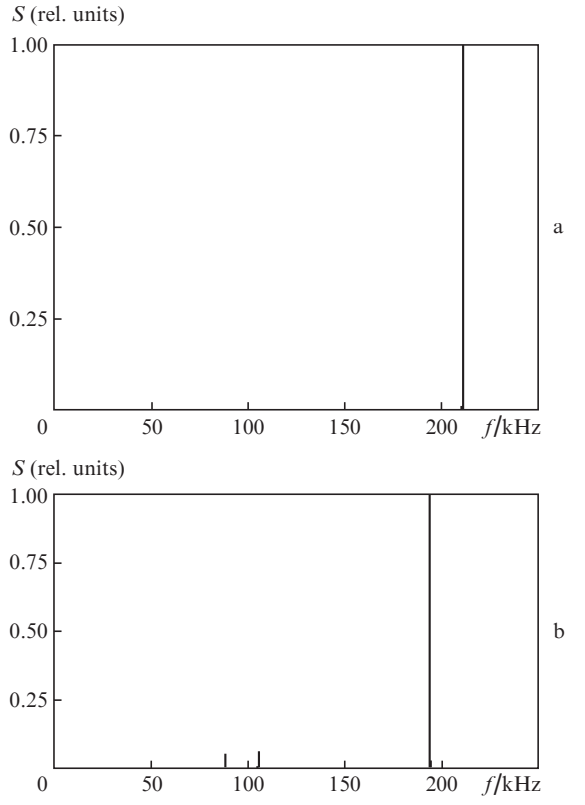

Figure 4. Experimentally measured radiation intensity spectra at $\eta_0 = 0.15$ for the periodic ($f_p = 210.4$ kHz) (a) and quasi-periodic ($f_p = 194$ kHz) (b) synchronisation regimes.

The typical experimentally measured radiation intensity spectra for the periodic and quasi-periodic regimes of synchronisation of SOs are shown in Fig. 4. In agreement with the numerical calculation results (see Fig. 1), the intensity spectra in the case of the periodic synchronisation regime (Fig. 4a) contain only one spectral component, which corresponds to the locked OS frequency ($f_m = f_p$). In the quasi-period regime (Fig. 4b), the radiation spectrum contains the main peak at the locked SO frequency and two small additional peaks, at the frequency f_1 (left peak) and at the combinations frequency $f_p - f_1$ (right peak).

Figure 5 shows the experimentally measured existence regions of the periodic and quasi-periodic synchronisation regimes at $\eta_0 = 0.15$ and 0.17 and the pump modulation depth $h = 0.25$. The presented experimental results qualitatively agree with the numerical simulation results (see Fig. 2): (1) the periodic regime is observed in the frequency region near f_+, while the quasi-periodic region exists near f_-; (2) the region of the quasi-periodic regime becomes wider with increasing pump excess over the threshold η_0; and (3) the experimentally measured frequencies of additional peaks f_1 are close to the corresponding peaks found by numerical simulation.

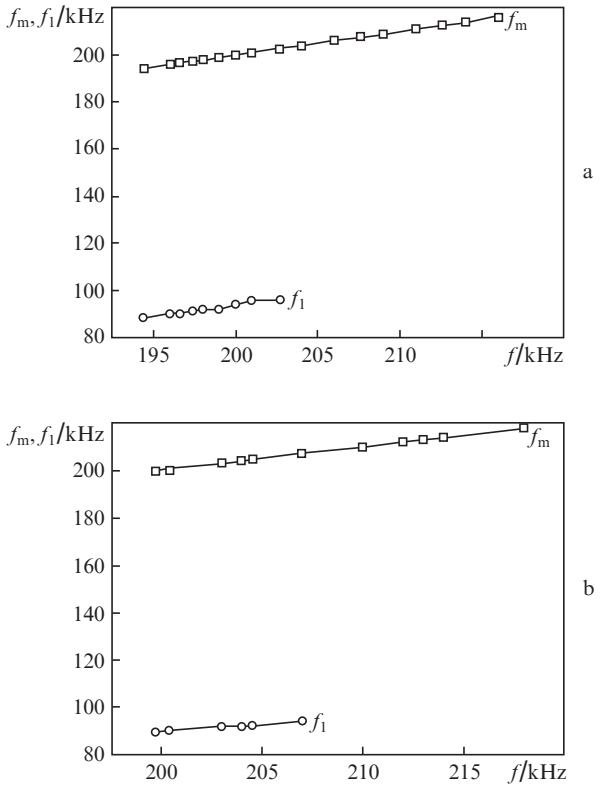

Figure 5. Experimentally measured existence regions of the periodic and quasi-periodic synchronisation regimes at the pump excess over the threshold $\eta_0 = 0.15$ (a) and 0.17 (b); the modulation depth is $h = 0.25$.

5. Synchronisation regime with a doubled period

5.1. Numerical simulation results

In the region of the pump excess over the threshold $0.2 \leqslant \eta_0 \leqslant 0.22$ in the absence of pump modulation ($h = 0$), the self-modulation regime of the first kind still remains stable. At

$h \neq 0$, we numerically found in this region two branches of bistable stabilisation of SOs. The periodic and quasi-periodic synchronisation regimes considered in Section 4 exist in the first branch, while, near the upper boundary of the existence region of the quasi-periodic synchronisation regime in a narrow (~1 kHz) range of the modulation signal frequencies f_p, one observes the synchronisation regime with a doubled modulation period (regime I) with the following characteristic features: the SO frequency is locked by the external signal ($f_m = f_p$) and an additional spectral component at the subharmonic frequency $f_p/2$ appears in the intensity spectrum. The radiation intensity spectrum in the synchronisation regime I is shown in Fig. 6a.

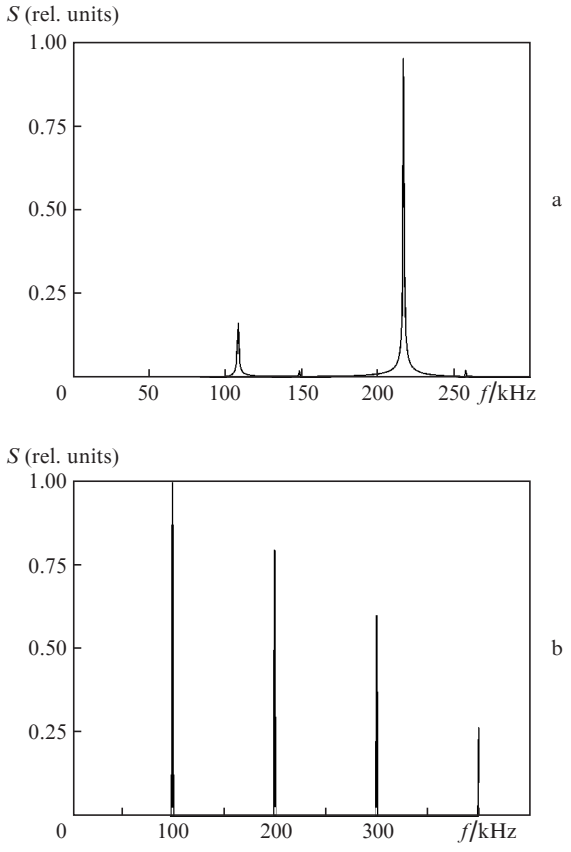

Figure 6. Numerically simulated radiation intensity spectra at $\eta_0 = 0.2$ and $h = 0.25$ for two branches of bistable synchronisation regimes with a double modulation period: the first branch (regime I), $f_p = 217$ kHz (a) and the second branch (regime II), $f_p = 200$ kHz (b).

Another synchronisation regime with a doubled period (regime II) is observed in the second branch at $0.2 \leqslant \eta_0 \leqslant 0.22$ and the pump modulation depth $h = 0.25$ in the entire synchronisation range (from $f_- = 184$ kHz to $f_+ = 220$ kHz). In this regime, several additional spectral components appear in the radiation intensity spectrum at the subharmonic frequency $f_p/2$ and multiple frequencies $kf_p/2$ ($k = 1, 2, 3\ldots$). A typical intensity spectrum in regime II at $f_p = 200$ kHz is shown in Fig. 6b.

5.2. Comparison with experiment

Experiments in the range of pump excess over the threshold $0.2 \leqslant \eta_0 < 0.22$ showed the existence of the periodic and quasi-periodic synchronisation regimes, while the synchronisation regime with a doubled period exists only in a narrow (~1 kHz) range of modulation frequencies f_p.

Figure 7 presents the experimentally measured radiation intensity spectrum for the synchronisation regime with a doubled period at $f_p = 214.5$ kHz, $\eta_0 = 0.2$, and $h = 0.25$. Comparing this spectrum with Fig. 2, one can see that the spectral shape is similar to that obtained by numerical simulation for the synchronisation regime I (the first branch of bistable synchronisation regimes). Unfortunately, we failed to experimentally observe the second branch of bistable regimes simulated numerically.

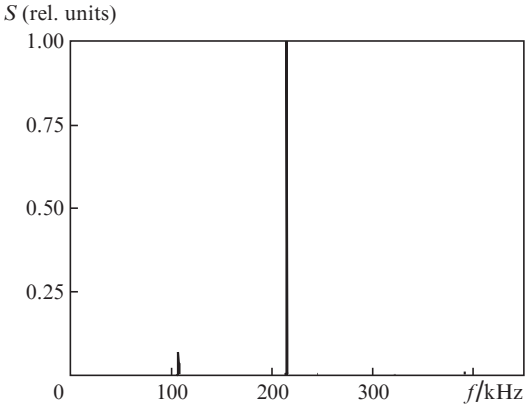

Figure 7. Experimentally measured radiation intensity spectrum for the synchronisation regime with a doubled period at $f_p = 214.5$ kHz, $\eta_0 = 0.2$, and $h = 0.25$.

6. Synchronisation of SOs with a doubled period

6.1. Numerical simulation results

At $\eta_0 \geqslant 0.22$, the self-modulation regime of the first kind in self-contained SSRLs becomes unstable and is replaced by a periodic self-modulation regime with a doubled period of oscillations of counterpropagating waves. Synchronisation of SOs by an external signal in this regime has not been previously studied. The numerical simulation performed in this study showed that, in the case of periodic pump modulation, the self-modulation regime with a doubled period can have two bistable branches of synchronisation of SOs. The first branch exhibits the periodic and quasi-periodic synchronisation regimes considered in Section 4. Figure 8 shows the radiation intensity spectra simulated for the first branch at $\eta_0 = 0.23$ in the absence of pump modulation and in the periodic synchronisation regime. At $h = 0$, the radiation intensity spectrum contains the spectral component at the $f_m/2$ subharmonic of the SO frequency, i.e., doubling of the oscillation period takes place (Fig. 8a). The first branch in the periodic synchronisation regime (Fig. 8b) shows only the spectral component at f_p, while the $f_p/2$ harmonic is absent. This indicates that the synchronisation in this case leads both to locking of the SO frequency and to a twofold decrease in the oscillation period. In the second branch, the spectral component at the subharmonic frequency $f_p/2$ exists in the entire synchronisation range and is close in amplitude to the main spectral component at f_p. Thus, the initial (existing before synchronisa-

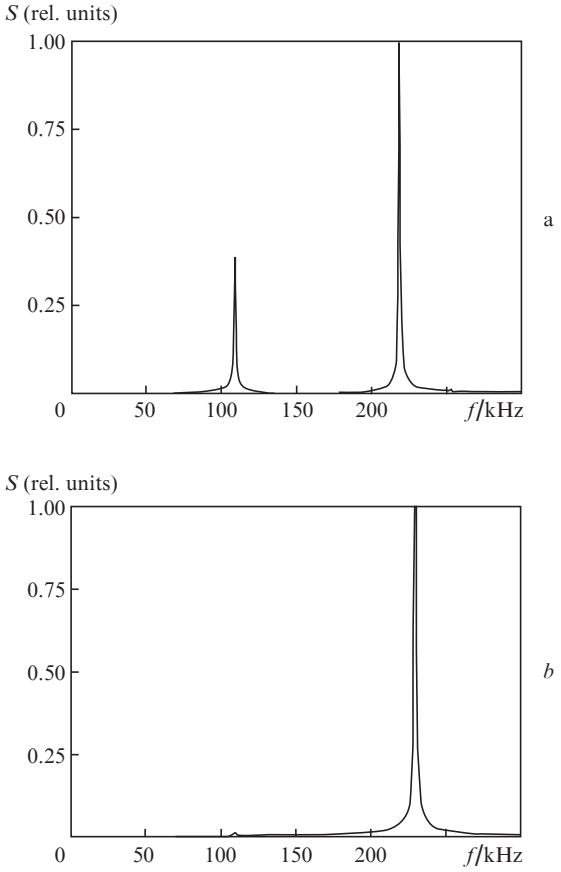

Figure 8. Numerically simulated radiation intensity spectra at $\eta_0 = 0.23$ in the absence of pump modulation (a) and in the periodic synchronisation regime in the first branch at $f_p = 230$ kHz and $h = 0.25$ (b).

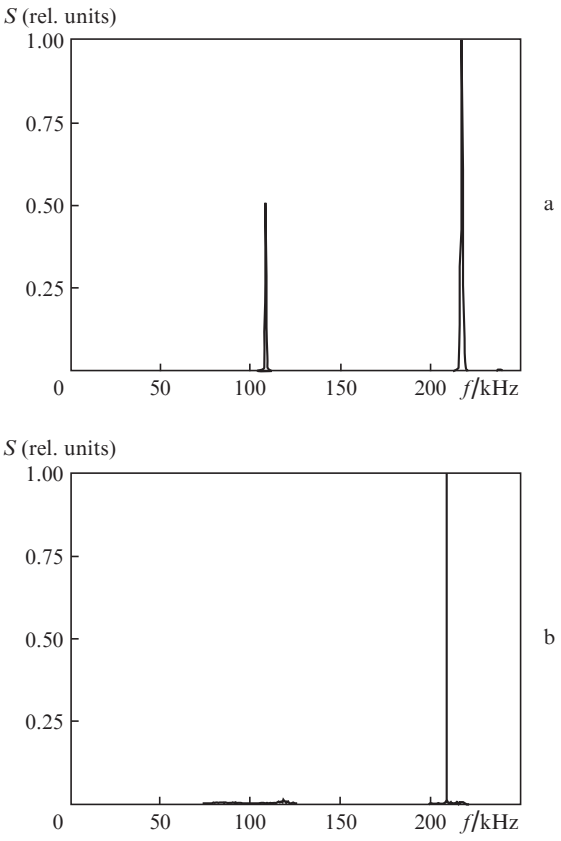

Figure 9. Experimentally measured radiation intensity spectra at $\eta_0 = 0.23$ in the absence of pump modulation (a) and in the periodic synchronisation regime at $f_p = 209$ kHz and $h = 0.25$ (b).

tion) doubling of the OS period is retained upon synchronisation in the second branch.

6.2. Comparison with experiment

Let us consider the experimental results obtained at $\eta_0 = 0.23$. Figure 9 shows the experimentally measured radiation intensity spectra in the absence of pump modulation and in the periodic synchronisation regime. In the first case, the laser operates in the self-modulation regime with a doubled period. Comparing the experimental data with the numerical simulation results, one can conclude that the experimentally observed synchronisation regimes belong to the first branch of the bistable regimes found by numerical simulation.

7. Conclusions

Thus, we studied frequency synchronisation for two self-modulation oscillation regimes (the regime of the first kind and the regime with a doubled period) existing in the parametric resonance region in the case of pump modulation by an external periodic signal. The comparison of the experimental and calculated results allows us to conclude that the vector model of an SSRL [8–14] is not completely adequate, since the experimental data qualitatively agree with the numerical simulation results only for one branch of bistable oscillation regimes. Synchronisation regimes for the other branch were not observed experimentally.

Acknowledgements. This work was supported by the Russian Foundation for Basic Research (Grant No. 11-02-00080).

References

1. Mendez J.M., Laje R., Giudici M., Aliaga J., Mindlin G.B. *Phys. Rev. E*, **63**, 066218 (2001).
2. Kravtsov N.V., Pashinin P.P., Sidorov S.S., Firsov V.V. *Kvantovaya Elektron.*, **32** (6), 562 (2002) [*Quantum Electron.*, **32** (6), 562 (2002)].
3. Kravtsov N.V., Lariontsev E.G., Pashinin P.P., Sidorov S.S., Firsov V.V. *Laser Phys.*, **13**, 305 (2003).
4. Pisarchik A.N., Barmenkov Yu.O. *Opt. Commun.*, **254**, 128 (2005).
5. Loose A., Wünsche H.J., Henneberger F. *Phys. Rev. E*, **82**, 035201 (2010).
6. Aulova T.V., Kravtsov N.V., Lariontsev E.G., Chekina S.N. *Kvantovaya Elektron.*, **41** (6), 504 (2011) [*Quantum Electron.*, **41** (6), 504 (2011)].
7. Pikovsky A., Rosenblum M., Kurths J. *Synchronization. A Universal Concept in Nonlinear Sciences* (Cambridge: Cambridge University Press, 2001).
8. Kravtsov N.V., Lariontsev E.G. *Kvantovaya Elektron.*, **36** (3), 192 (2006) [*Quantum Electron.*, **36** (3), 192 (2006)].
9. Schwartz S., Feugnet G., Lariontsev E.G., Pocholle J.P. *Phys. Rev. A*, **76**, 023807 (2007).
10. Zolotoverkh I.I., Kamysheva A.A., Kravtsov N.V., Lariontsev E.G., Firsov V.V., Chekina S.N. *Kvantovaya Elektron.*, **38** (10), 956 (2008) [*Quantum Electron.*, **38** (10), 956 (2008)].

11. Aulova T.V., Kravtsov N.V., Lariontsev E.G., Chekina S.N. *Kvantovaya Elektron*., **41** (1), 13 (2011) [*Quantum Electron*., **41** (1), 13 (2011)].
12. Zolotoverkh I.I., Klimenko D.N., Lariontsev E.G. *Kvantovaya Elektron*., **23** (7), 625 (1996) [*Quantum Electron*., **26** (7), 604 (1996)].
13. Zolotoverkh I.I., Kravtsov N.V., Kravtsov N.N., Lariontsev E.G., Makarov A.A. *Kvantovaya Elektron*., **24** (7), 638 (1997) [*Quantum Electron*., **27** (7), 621 (1997)].
14. Zolotoverkh I.I., Kravtsov N.V., Lariontsev E.G., Firsov V.V., Chekina S.N. *Kvantovaya Elektron*., **37** (11), 1011 (2007) [*Quantum Electron*., **37** (11), 1011 (2007)].